

Isotope effects in the CO dimer: Millimeter wave spectrum and rovibrational calculations of ($^{12}\text{C}^{18}\text{O}$)₂

L. A. Surin, D. N. Fourzikov, T. F. Giesen, S. Schlemmer, and G. Winnewisser
I. Physikalisches Institut, Universität zu Köln, Zùlpicher Str. 77, 50937 Cologne, Germany

V. A. Panfilov and B. S. Dumesh
Institute of Spectroscopy, Russian Academy of Sciences, 142190 Troitsk, Moscow Region, Russia

G. W. M. Vissers
Department of Chemistry, The Ohio State University, Columbus, Ohio 43210

A. van der Avoird^{a)}
Institute of Theoretical Chemistry, IMM, Radboud University Nijmegen, Toernooiveld 1, 6525 ED Nijmegen, The Netherlands

(Received 30 May 2006; accepted 2 August 2006; published online 1 September 2006)

The millimeter wave spectrum of the isotopically substituted CO dimer, ($^{12}\text{C}^{18}\text{O}$)₂, was studied with the Orotron jet spectrometer, confirming and extending a previous infrared study [A. R. W. McKellar, *J. Mol. Spectrosc.* **226**, 190 (2004)]. A very dilute gas mixture of CO in Ne was used, which resulted in small consumption of $^{12}\text{C}^{18}\text{O}$ sample gas and produced cold and simple spectra. Using the technique of combination differences together with the data from the infrared work, six transitions in the 84–127 GHz region have been assigned. They belong to two branches, which connect four low levels of A^+ symmetry to three previously unknown levels of A^- symmetry. The discovery of the lowest state of A^- symmetry, which corresponds to the projection $K=0$ of the total angular momentum J onto the intermolecular axis, identifies the geared bending mode of the $^{12}\text{C}^{18}\text{O}$ dimer at 3.607 cm^{-1} . Accompanying rovibrational calculations using a recently developed hybrid potential from *ab initio* coupled cluster [CCSD(T)] and symmetry-adapted perturbation theory calculations [G. W. M. Vissers *et al.*, *J. Chem. Phys.* **122**, 054306 (2005)] gave very good agreement with experiment. The isotopic dependence of the A^+/A^- energy splitting, the intermolecular separation R , and the energy difference of two ground state isomers, which change significantly when ^{18}O or ^{13}C are substituted into the normal ($^{12}\text{C}^{16}\text{O}$)₂ isotopolog [L. A. Surin *et al.*, *J. Mol. Spectrosc.* **223**, 132 (2004)], was explained by these calculations. It turns out that the change in anisotropy of the intermolecular potential with respect to the shifted monomer centers of mass is particularly significant. © 2006 American Institute of Physics.
 [DOI: [10.1063/1.2345202](https://doi.org/10.1063/1.2345202)]

I. INTRODUCTION

During the last years significant experimental progress has been achieved in understanding the previously mysterious spectra of the carbon monoxide dimer as well as its energy level pattern. Following the pioneering but inconclusive 1979 microwave results of Vanden Bout *et al.*,¹ a series of infrared and millimeter wave spectroscopic studies of ($^{12}\text{C}^{16}\text{O}$)₂ (Refs. 2–10) were carried out. The results are summarized in a recent paper.¹¹ There has also been parallel progress^{12,13} in understanding the structure and dynamics of (CO)₂ by means of accurate *ab initio* calculations of the potential energy surface, which appear to be especially difficult for this system,^{14–20} combined with calculations of its rovibrational states.

It was experimentally established that the rotational levels of the CO dimer occur in “stacks” with well defined values of K ($=0, 1, 2$), the quantum number for the projection of the total angular momentum J on the intermolecular axis.

The intermolecular axis is the vector \mathbf{R} from the center of mass of one CO monomer to that of the other CO monomer. Each stack of rotational levels has been given an arbitrary label, a, b, c, \dots . The CO dimer is a floppy system with permutation-inversion (PI) group G_4 generated by the interchange of the two identical monomers and inversion.^{21,22} This group has the irreducible representations (irreps) A^\pm and B^\pm , where the \pm parity label denotes the inversion symmetry. For standard ($^{12}\text{C}^{16}\text{O}$)₂ isotopolog the B^\pm symmetry are Pauli forbidden (they have nuclear spin statistical weight zero) because both ^{12}C and ^{16}O are bosons with zero nuclear spin. Hence, the rovibrational states of the $^{12}\text{C}^{16}\text{O}$ dimer can be classified as having either A^+ or A^- PI symmetry.

A remarkable feature of the energy level scheme is the apparent presence of two isomers in the form of two low-lying A^+ stacks with $K=0$ (the ground a state and the excited c state at 0.88 cm^{-1}). Recent theoretical calculations^{12,13} have shed much light on this problem. It was found that both isomers are planar with slipped antiparallel structures (see Fig. 1). The a state corresponds to the global minimum in the

^{a)}Electronic mail: avda@theochem.kun.nl

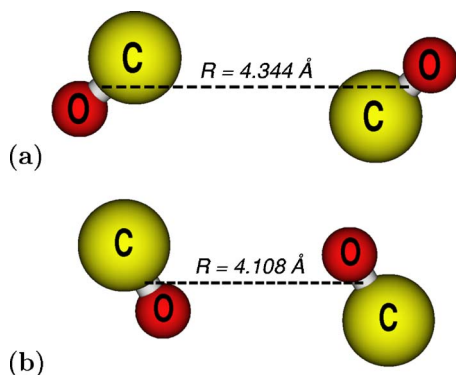


FIG. 1. Equilibrium structures of the CO dimer corresponding to the global minimum in the potential surface with a relatively large equilibrium distance R_e [panel (a)] and to the local minimum with a much smaller value of R_e [panel (b)].

calculated potential energy surface with the C atoms closer to each other than the O atoms [see Fig. 1(a)]. The C atoms have a larger van der Waals radius than the O atoms, so the distance R between the centers of mass of the monomers is relatively large in this equilibrium geometry. The c state corresponds to a local minimum in the intermolecular potential where the O atoms are closer together, and the distance R between the monomers is much smaller [see Fig. 1(b)]. There is also A^+/A^- symmetry splitting (formerly believed to be a tunneling splitting), represented by the separation between the A^+ ground state (the a state) and the lowest A^- stack (the e state at 3.73 cm^{-1} with $K=0$). The *ab initio* studies^{12,13} have shown that this A^+/A^- separation corresponds to an antisymmetric vibration or geared bending motion of the complex. The very low excitation frequency indicates that the dimer is indeed very floppy.

Usually for such floppy dimers one finds tunneling between equivalent minima. In the equilibrium geometry of the dimer the two monomers are inequivalent, and tunneling interchanges the monomers. See, for example, work on HF–HF (Refs. 23 and 24) and HCl–HCl,²⁵ as well as on the water dimer.^{26,27} In all these hydrogen bonded complexes there is a tunneling process that interchanges the donor and the acceptor in the hydrogen bond. In the case of the CO dimer the point group C_{2h} of each equilibrium structure is isomorphic to the PI group G_4 , so there is no interchange tunneling at either of the two minima. The two minima are separated by an energy barrier, and without tunneling there would be two vibrational ground state wave functions corresponding to two “isomers” localized in either one of the wells (corresponding to the stacks a and c). Calculations on the *ab initio* potential computed by the coupled cluster method with singly and doubly excited states and perturbative inclusion of triples¹² [CCSD(T)], and on the potential obtained from symmetry-adapted perturbation theory with monomer wave functions from density functional theory¹³ (SAPT-DFT) indeed produced such a situation of two isomers localized in either of the two potential wells. However, the relative energies of these a and c isomers did not agree with experiment; nor did the vibrationally averaged intermolecular distances R . Also the energies of the higher stacks showed rather large discrepancies relative to the experimental data, and the shifts pre-

dicted when ^{12}C was substituted by ^{13}C were completely wrong. Then a hybrid intermolecular potential energy surface was devised as a weighted average of the two potentials from CCSD(T) and SAPT-DFT, with an empirically determined weighting coefficient.¹³ The weighting coefficient [0.7 for the CCSD(T) potential and 0.3 for the SAPT-DFT potential] was fixed such that the observed small energy difference of 0.88 cm^{-1} between the a and c states was correctly reproduced. This hybrid potential gives results in very good agreement with the experimental data, for both $(^{12}\text{C}^{16}\text{O})_2$ and $(^{13}\text{C}^{16}\text{O})_2$. The CO dimer wave functions that were computed with this hybrid potential are, to some extent, delocalized over the two minima (see Ref. 13). Obviously, the experimental data can only be explained when this delocalization is taken into account in the calculations. This holds in particular for the isotope shifts, to be discussed below. The observed isotope effects for $(^{13}\text{C}^{16}\text{O})_2$ relative to $(^{12}\text{C}^{16}\text{O})_2$ were explained by a stronger localization of the wave functions in either one of two wells due to the larger mass of the molecules.

The delocalization of the lowest two eigenstates of the rovibrational Hamiltonian implies that the system tunnels between the two potential wells through the barrier that separates these wells. Hence, one finds in the case of the CO dimer that tunneling occurs between two *inequivalent* minima in the intermolecular potential surface. This is directly related to the fact that the D_0 energy difference between the a and c isomers is extremely small: 0.88 cm^{-1} , which is the more striking since the global and local minima differ by as much as 16 cm^{-1} in depth D_e (in the hybrid potential). This difference in D_e is almost completely compensated by the larger zero-point vibrational energy in the global minimum (which has a narrower well than the local minimum).

On the experimental side, one avenue towards a more complete understanding of the CO dimer is the study of isotopically substituted species. Thus, the infrared²⁸ and millimeter wave²⁹ spectra of $(^{13}\text{C}^{16}\text{O})_2$ have been studied in some detail, and there is also limited data for the mixed dimer, $^{12}\text{C}^{16}\text{O}-^{13}\text{C}^{16}\text{O}$.^{5,30} More recently, the infrared spectrum of the $^{12}\text{C}^{18}\text{O}$ dimer was also observed.³¹ The present paper reports the first millimeter wave study of this $(^{12}\text{C}^{18}\text{O})_2$ isotopolog in the frequency range of 84–127 GHz. These results lead to a considerable extension of the previous analysis of this isotopolog, which was based on its infrared spectrum.³¹ The lowest stack of A^- symmetry was discovered, in addition to the two stacks of A^+ symmetry determined earlier.³¹ The infrared spectra of $(^{13}\text{C}^{16}\text{O})_2$ (Ref. 28) and $(^{12}\text{C}^{18}\text{O})_2$ (Ref. 31) and the millimeter wave spectrum of $(^{13}\text{C}^{16}\text{O})_2$ (Ref. 29) showed already that the results were sufficiently similar to $(^{12}\text{C}^{16}\text{O})_2$ to label the energy level stacks with the same scheme. As already mentioned, in the normal isotope of the CO dimer, $(^{12}\text{C}^{16}\text{O})_2$, all the nuclei have zero spin and only half of the normally expected rotational levels are allowed; levels may have either A^+ or A^- symmetry.¹⁵ Exactly the same nuclear spin statistics apply to $(^{12}\text{C}^{18}\text{O})_2$, the subject of this paper. By contrast, ^{13}C has a nuclear spin of $\frac{1}{2}$ and the statistics for $(^{13}\text{C}^{16}\text{O})_2$ are different,^{28,29} with the

result that the A^+ and A^- levels (with statistical weight of 1) are joined by new B^+ and B^- levels (with statistical weight of 3).

The small differences induced by isotopic substitution constitute a subtle probe of the CO intermolecular dynamics. Interestingly, the energy spacing between the two lowest stacks a and c (corresponding to the two isomers) was found to be larger for $(^{13}\text{C}^{16}\text{O})_2$ but smaller for $(^{12}\text{C}^{18}\text{O})_2$ [1.29 Ref. 28 and 0.64 Ref. 31 as compared to 0.88 cm^{-1} Ref. 5 for the normal isotopolog]. The A^+/A^- energy splitting for $(^{12}\text{C}^{18}\text{O})_2$ determined in the present study to be 3.61 cm^{-1} is smaller than for the normal isotopolog [3.73 cm^{-1} Ref. 6], whereas for $(^{13}\text{C}^{16}\text{O})_2$ [3.77 cm^{-1} Ref. 29] it is larger. Also the intermolecular distance R , which for each isotopolog is defined as the distance between the centers of mass of the corresponding monomers, shows opposite shifts with ^{13}C (Ref. 28) and ^{18}O (Ref. 31) substitution. One might think that such opposite shifts in R are a consequence of the shift of the monomer centers of mass in the dimer equilibrium geometries, but it was shown for $(^{12}\text{C}^{16}\text{O})_2$ and $(^{13}\text{C}^{16}\text{O})_2$ in Refs. 12 and 13 that this “static” shift in R differs both in magnitude and direction from the experimentally observed shift. The opposite shifts in the various properties of the two heavier isotopologs seem to be inconsistent with the fact that both $^{12}\text{C}^{18}\text{O}$ and $^{13}\text{C}^{16}\text{O}$ have a larger mass and a smaller rotational constant than $^{12}\text{C}^{16}\text{O}$. In order to explain this behavior new rovibrational calculations were made based on the hybrid potential.¹³ These are described in Secs. IV and V, while the experiments are presented in Secs. II and III.

II. EXPERIMENTAL DETAILS

The millimeter wave spectra of the $^{12}\text{C}^{18}\text{O}$ dimer were measured in some selected frequency ranges from 84 to 127 GHz using the intracavity jet spectrometer, Orotron. Details of the setup are given elsewhere.³² Briefly, the homemade millimeter wave generator Orotron is placed in the vacuum chamber together with the supersonic jet apparatus. The molecular beam is injected into the Orotron cavity perpendicularly to its axis. The high Q factor of the cavity results in 100 effective passes of the radiation through the jet. Absorption in the cavity causes changes of the electron current in the collector circuit of the Orotron and is detected very sensitively by measuring these current changes. A small part of the millimeter wave radiation is taken out of the cavity through coupling openings in a spherical mirror and is mixed with the radiation of the HP 8671B microwave synthesizer for frequency determinations.

The experiment was performed with a pinhole pulsed jet source (General Valve, series 9). The diameter of the nozzle was 0.8 mm, and the typical repetition rates were 10–15 Hz. The pumping system utilized an Edwards 9B3K booster pump and, as backing, a Pfeiffer DUO 20M rotary pump. We used a gas mixture of 1% of $^{12}\text{C}^{18}\text{O}$ in Ne at a backing pressure of 3.5 bars. Such a dilute gas mixture resulted in small consumption of the $^{12}\text{C}^{18}\text{O}$ sample gas as well as cold and simple spectra. For most of the absorption measure-

TABLE I. Observed $K=0\rightarrow 0$ millimeter wave $P(J)=J\rightarrow J-1$ and $R(J)=J\rightarrow J+1$ transitions of the $^{12}\text{C}^{18}\text{O}$ dimer ($a\rightarrow e$ subband).

| $K=0\rightarrow 0$ $a\rightarrow e$ | Frequency (MHz) |
|----------------------------------------|--------------------|
| $P(2)$ | 100 961.923 |
| $P(4)$ | 94 545.555 |
| $P(6)$ | 89 535.377 |
| $R(0)$ | 111 745.131 |
| $R(2)$ | 118 962.546 |
| $R(4)$ | 126 726.756 |

ments, the full linewidth at half height (FWHH) is about 300 kHz and the accuracy of line center positions is estimated to be about 50 kHz.

III. EXPERIMENTAL RESULTS AND ANALYSIS

The initial search for the millimeter wave transitions of the $^{12}\text{C}^{18}\text{O}$ dimer was based on the energies of the lowest a and c stacks known from the infrared work³¹ and the presumption that the general pattern of the $(^{12}\text{C}^{18}\text{O})_2$ energy levels is similar to that of $(^{12}\text{C}^{16}\text{O})_2$ and $(^{13}\text{C}^{16}\text{O})_2$. But since all infrared ground state energy levels have A^+ symmetry, transitions among them are not allowed and they do not directly predict any millimeter wave positions. Rather, they contain combination differences which must also appear in the millimeter wave spectrum. Thus, for example, if we suspected that a certain millimeter wave line was an $R(0)$ transition, we could predict the position of a possible $P(2)$ line from the energies of the appropriate $J=2$ levels which were already known to infrared accuracy.³¹ In this way it was possible to put together a number of millimeter wave line assignments that were consistent with the infrared results.

The assignment resulted in the positive identification of transitions involving a new upper stack of levels with A^- symmetry in combination with the known a stack of A^+ symmetry. Based on its energy, it was reasonable to identify this new stack as the e stack with $K=0$, which was already known for $(^{12}\text{C}^{16}\text{O})_2$ and $(^{13}\text{C}^{16}\text{O})_2$. The assignment of the e state is especially important since this gives the lowest energy stack with A^- symmetry, and hence establishes the frequency of the lowest intermolecular mode of the dimer that we now know undoubtedly to be the geared bending mode.

The assigned millimeter wave transitions of $(^{12}\text{C}^{18}\text{O})_2$ are listed in Table I. The measurement uncertainty is better than 50 kHz. These data were combined in a least-squares term value analysis to determine a consistent set of energy levels, as given in Table II. Since the energies come from a term value analysis, they are almost entirely model independent. One of the observed lines, namely, the $a\rightarrow e$ $R(2)$ line, is displayed in Fig. 2. No transitions were observed from the c state to the e state in spite of an extensive search.

The energy levels determined here for the a state (Table II) may be directly compared with the earlier infrared results (Table III of Ref. 31). For the four independent levels the agreement is perfect, with the worst deviation of 0.0004 cm^{-1} for the $J=6$ level.

TABLE II. Energy levels of the $^{12}\text{C}^{18}\text{O}$ dimer (in cm^{-1}) from the experimental data.

| J | State a $A^+, K=0$ | State c^a $A^+, K=0$ | State e $A^-, K=0$ |
|-----|-------------------------|---------------------------|-------------------------|
| 0 | 0.0 | 0.6386 | |
| 1 | | | 3.727 417 |
| 2 | 0.359 689 | 1.0450 | |
| 3 | | | 4.327 852 |
| 4 | 1.174 152 | 2.0157 | |
| 5 | | | 5.401 302 |
| 6 | 2.414 723 | | |

^aAs determined by McKellar in the infrared study (Ref. 31).

The stacks were then rotationally analyzed in terms of their stack origins, rotational constants B , and centrifugal distortion constants D in the same way as was done previously for $(^{12}\text{C}^{16}\text{O})_2$ [Refs. 5–9] and $(^{13}\text{C}^{16}\text{O})_2$ [Refs. 28 and 29] using the following simple expression: Energy=Origin + $BJ(J+1) - DJ^2(J+1)^2$. The states a and c were treated as pairs connected by Coriolis-type interactions with the Coriolis coupling parameter W_C defined in Refs. 5 and 28. Because the present data for the e stack are somewhat limited, it was necessary to fix the distortion constant D of this stack at the value determined for $(^{12}\text{C}^{16}\text{O})_2$. The results are shown in Table III, which includes parameters for the a , c , and e states. The parameters for the a state differ slightly from those determined previously³¹ due to the more accurate measurement of the energy levels in the millimeter wave experiment. The table also includes values for the effective intermolecular separations $R_{\text{eff}}=(2\mu B)^{-1/2}$ for each stack determined directly from the fitted B values. These separations are used as the horizontal axis for the energy level diagram in Fig. 3.

In order to compare results for different CO dimer isotopologs it is useful to use the values of R_{eff} rather than the rotational constants B , since most of the differences in the latter are due simply to changes in the reduced mass. Figure 3 illustrates how the energies and R_{eff} values of the a , b , c , and e states change in going from $(^{12}\text{C}^{16}\text{O})_2$ (squares) to $(^{13}\text{C}^{16}\text{O})_2$ (circles) and to $(^{12}\text{C}^{18}\text{O})_2$ (triangles). Here the zero point of energy is placed halfway between the origins of the a and c states. This figure shows an extension of the trend

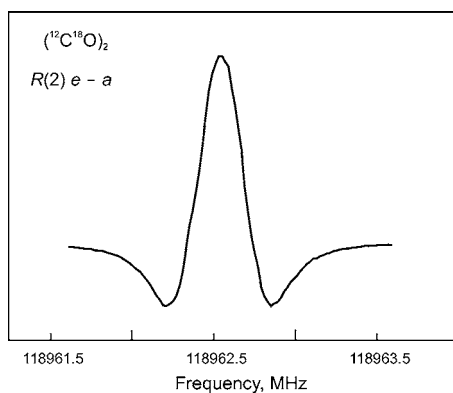


FIG. 2. Observed $R(2)$ transition of the $^{12}\text{C}^{18}\text{O}$ dimer belonging to the $a \rightarrow e$ band.

TABLE III. Empirical parameters for the observed states of the $^{12}\text{C}^{18}\text{O}$ dimer: B and D are the rotational and distortion constants, respectively, W_C is the Coriolis coupling parameter, (Refs. 5 and 28), and $R_{\text{eff}}=(2\mu B)^{-1/2}$.

| | State a $A^+, K=0$ | State c $A^+, K=0$ | State e $A^-, K=0$ |
|-----------------------------|-------------------------|----------------------------|-------------------------|
| Origin/ cm^{-1} | 0.0 | 0.638 62(20) | 3.607 78(82) |
| B/cm^{-1} | 0.060 592(10) | 0.067 100(44) | 0.060 056(42) |
| D/cm^{-1} | | $3.17(85) \times 10^{-6}$ | $8.8 \times 10^{-6}^a$ |
| W_C/cm^{-1} | | $8.555(64) \times 10^{-3}$ | |
| $R_{\text{eff}}/\text{\AA}$ | 4.307 | 4.093 | 4.326 |

^aFixed at value of normal isotopolog (Ref. 9)

previously noted^{28,29} when comparing $(^{12}\text{C}^{16}\text{O})_2$ and $(^{13}\text{C}^{16}\text{O})_2$, namely, when the separation of isomeric pairs of levels a/c increases, then the isotope shifts of their intermolecular separations R_{eff} also increase, and vice versa.

IV. ROVIBRATIONAL CALCULATIONS

As in Refs. 12 and 13, we define the geometry of the CO dimer consisting of molecules A and B by the four coordinates R , θ_A , θ_B , and ϕ . The intermolecular distance R is the length of the vector \mathbf{R} from the center of mass of monomer A to that of monomer B ; θ_A and θ_B are the angles between \mathbf{R} and the vectors \mathbf{r}_A and \mathbf{r}_B pointing from the C atom to the O atom in the monomers; and ϕ is the dihedral angle between the planes defined by $(\mathbf{R}, \mathbf{r}_A)$ and $(\mathbf{R}, \mathbf{r}_B)$.

The potential energy surface used in the calculations was the hybrid potential energy surface introduced in Ref. 13. This potential shows two minima close in energy, both corresponding to planar slipped antiparallel structures. The global minimum at -139 cm^{-1} corresponds to a structure where the C atoms are closer together [see Fig. 1(a)], the second minimum 16 cm^{-1} higher in energy to a similar structure with the O atoms nearest to each other [see Fig. 1(b)]. Due to zero-point energy effects the rovibrational energies of the lowest two states that are more or less localized at these two minima are very close: the energy difference is only 0.89 cm^{-1} for the $(^{12}\text{C}^{16}\text{O})_2$ dimer.

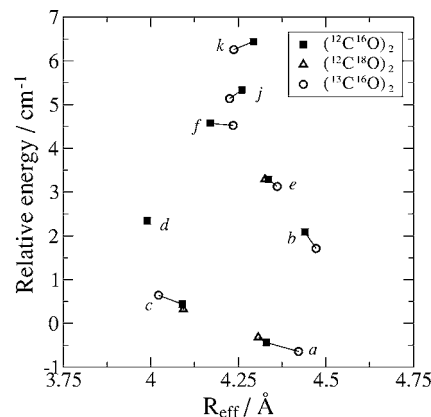


FIG. 3. Plot illustrating the isotopic dependence of the energies and intermolecular separations R_{eff} for various states of the CO dimer. The solid squares represent $(^{12}\text{C}^{16}\text{O})_2$ (Refs. 5 and 9), the open circles represent $(^{13}\text{C}^{16}\text{O})_2$ (Refs. 28 and 29), and the open triangles represent $(^{12}\text{C}^{18}\text{O})_2$ (Ref. 31 and the present work).

TABLE IV. Calculated parameters characterizing rotational stacks for the $^{12}\text{C}^{18}\text{O}$ dimer: B and D are the rotational and distortion constants, and $R_{\text{eff}}=(2\mu B)^{-1/2}$.

| Stack | K | Symmetry | R_{eff} (Å) | Origin (cm^{-1}) | B (cm^{-1}) | D (cm^{-1}) |
|----------|-----|----------|----------------------|-----------------------------|--------------------------|--------------------------|
| <i>a</i> | 0 | A^+ | 4.31 | 0.00 | 0.060 427 | 6.3×10^{-5} |
| <i>b</i> | 1 | A^+ | 4.62 | 2.46 | 0.052 761 | -2.6×10^{-5} |
| <i>c</i> | 0 | A^+ | 4.12 | 0.64 | 0.066 288 | -5.7×10^{-5} |
| <i>d</i> | 1 | A^+ | 3.79 | 2.21 | 0.078 144 | 1.4×10^{-4} |
| <i>e</i> | 0 | A^- | 4.29 | 3.43 | 0.061 074 | 1.6×10^{-5} |
| <i>f</i> | 1 | A^- | 4.27 | 4.99 | 0.061 722 | -2.0×10^{-5} |
| <i>g</i> | 1 | A^+ | 4.12 | 7.87 | 0.066 229 | 9.2×10^{-5} |
| <i>j</i> | 0 | A^- | 4.31 | 5.34 | 0.060 590 | -2.6×10^{-5} |
| <i>k</i> | 1 | A^- | 4.32 | 6.61 | 0.060 348 | -1.7×10^{-5} |

The centers of mass in the $^{12}\text{C}^{18}\text{O}$ molecules are shifted slightly compared to $^{12}\text{C}^{16}\text{O}$. To account for this effect, the coordinates for the $^{12}\text{C}^{18}\text{O}$ dimer were transformed to coordinates describing the same geometry in the $^{12}\text{C}^{16}\text{O}$ dimer, and the potential of $(^{12}\text{C}^{16}\text{O})_2$ was reexpanded in terms of coupled angular functions [see Eq. (7) of Ref. 13] in the new coordinates.

The methodology for the rovibrational calculations is the same as in Refs. 12 and 13, and the parameters and basis sets were the same as those used in the calculations on $(^{12}\text{C}^{16}\text{O})_2$ and $(^{13}\text{C}^{16}\text{O})_2$. Rovibrational states of A^+ and A^- symmetries were calculated for total angular momentum $J=0, \dots, 6$, taking Coriolis coupling into account. Although K , the projection of the total angular momentum J on R , is strictly not a good quantum number, we found that for nearly all computed states the contribution of one particular K value was dominant. As in the experiment, the calculated energy levels were fit to a simple rigid rotor expression. The resulting parameters are given in Table IV.

In order to facilitate comparison with the experimental data, a graphical representation of the shifts of the stack origins upon substitution of ^{16}O by ^{18}O is given in Fig. 4. The previously calculated¹³ effect of substituting ^{12}C by ^{13}C is also drawn in this figure. For all three isotopologs, the zero point of energy is chosen halfway between the *a* and *c* stack

origins. It is obvious from Figs. 3 and 4 that theory and experiment agree very well on the effect of both isotopic substitutions, for all stacks observed.

V. DISCUSSION

It was shown in Ref. 13 that due to tunneling between the two nearly degenerate potential energy wells the wave functions of $(^{12}\text{C}^{16}\text{O})_2$ are to some extent delocalized over the two well regions. It was demonstrated, (see Figs. 10 and 11 of Ref. 13) that the effect of substituting ^{12}C with ^{13}C can be understood in terms of a loss of this delocalization of the wave functions due to the larger mass and rotational constant of the $^{13}\text{C}^{16}\text{O}$ molecules.¹² One would therefore expect the wave functions of the $^{12}\text{C}^{18}\text{O}$ dimer to exhibit a similar loss of delocalization, and its rovibrational stacks to have similar isotope shifts with respect to their $^{12}\text{C}^{16}\text{O}$ counterparts as found for the $^{13}\text{C}^{16}\text{O}$ dimer. As can be seen in Fig. 4 this is not the case. For most of the stacks, the effect of substituting the ^{16}O atom by a heavier ^{18}O isotope is opposite to that of replacing the ^{12}C atom with ^{13}C . Also, the wave functions of the $^{12}\text{C}^{18}\text{O}$ dimer in Fig. 5 show, if anything, more delocalization over the two minima rather than less. In order to investigate this further, we also computed the *a* and *c* stack energy levels for $(^{12}\text{C}^{18}\text{O})_2$ and $(^{13}\text{C}^{16}\text{O})_2$ with the potential energy surface expressed in the coordinates, R , θ_A , θ_B , and ϕ , of $(^{12}\text{C}^{16}\text{O})_2$, without adjusting these coordinates for the shift in the monomer centers of mass. The results are summarized in Table V.

One can see that when the coordinates in which the potential is expressed are not adjusted for the shift in the monomer centers of mass, i.e., when the anisotropy of the potential with respect to the monomer centers of mass is kept the same as in $(^{12}\text{C}^{16}\text{O})_2$, the $^{12}\text{C}^{18}\text{O}$ dimer shows much the same trends as the $^{13}\text{C}^{16}\text{O}$ dimer: the energy difference between the *a* and *c* stacks becomes larger in both cases, and the difference between the R_{eff} values for the *a* and *c* stacks increases. Comparing the results for the $^{13}\text{C}^{16}\text{O}$ dimer with and without accounting for the changed anisotropy of the potential with respect to $(^{12}\text{C}^{16}\text{O})_2$, we see that the changes in monomer mass and rotational constant do not account completely for the observed isotope effect. The slight change in the anisotropy of the potential caused by the center of mass shift also plays a role. This is confirmed by the results for the $^{12}\text{C}^{18}\text{O}$ dimer. Whereas the effects caused by the total

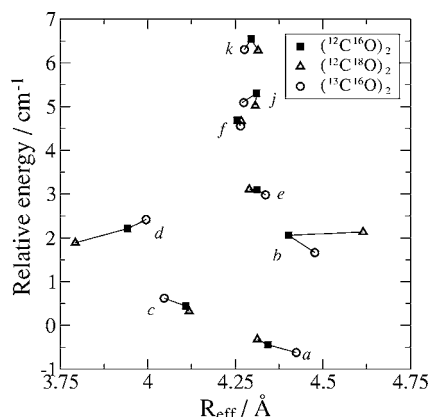


FIG. 4. Calculated relative energies of the stack origins vs intermolecular separation R_{eff} for $(^{12}\text{C}^{16}\text{O})_2$, $(^{13}\text{C}^{16}\text{O})_2$, and $(^{12}\text{C}^{18}\text{O})_2$. For each of the isotopologs the zero point of energy is chosen halfway between the *a* and *c* stack origins.

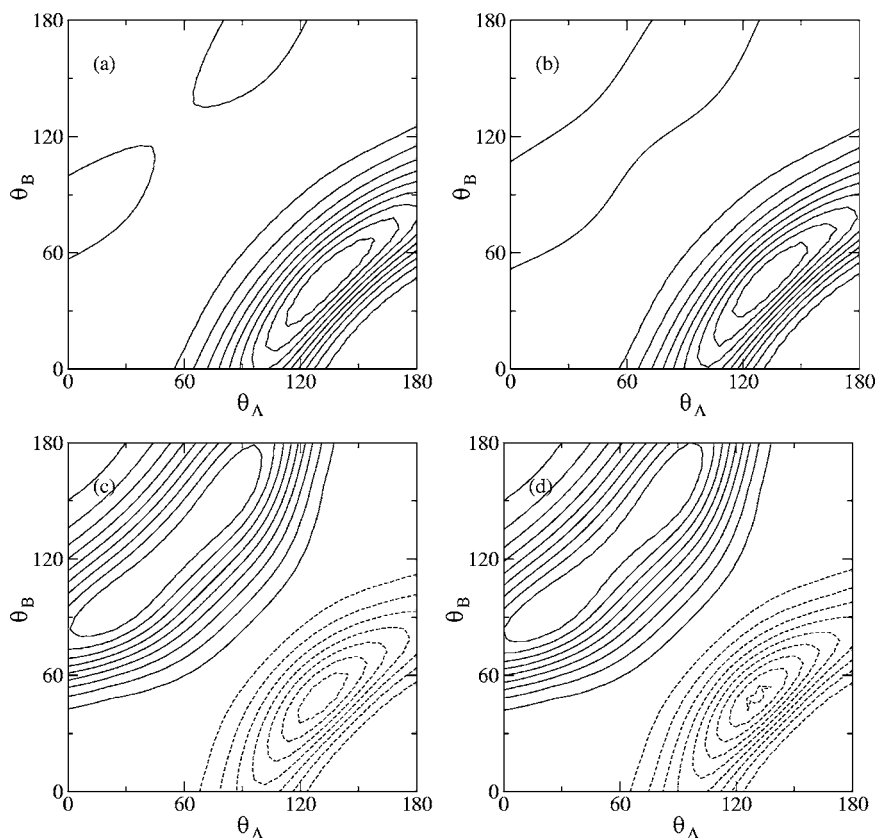


FIG. 5. Cuts through the wave functions of the lowest level of (a) the a stack of $(^{12}\text{C}^{16}\text{O})_2$, (b) the a stack of $(^{12}\text{C}^{18}\text{O})_2$, (c) the c stack of $(^{12}\text{C}^{16}\text{O})_2$, and (d) the c stack of $(^{12}\text{C}^{18}\text{O})_2$. The cuts are for $\phi=180^\circ$ and $R=R_{\text{eff}}$.

and reduced monomer masses are in the same direction as for the ^{13}C substituted dimer, the total isotope effect on the a/c energy gap and rotational constants B of the a and c stacks is in the opposite direction. This can be explained by the fact that the $^{12}\text{C}^{16}\text{O}$ center of mass shifts towards the O atom upon substitution by ^{18}O , but towards the C atom upon ^{13}C substitution. In the $^{12}\text{C}^{18}\text{O}$ dimer, the effect of the larger monomer mass is canceled and even reversed by the effect of the anisotropy of the potential caused by the monomer center of mass shift.

VI. CONCLUSION

We studied the millimeter wave spectrum of the isotopically substituted CO dimer, $(^{12}\text{C}^{18}\text{O})_2$. The experiment was performed using a pulsed supersonic jet expansion and intracavity Orottron spectrometer. The results confirm and extend a previous infrared study.³¹ A total of seven new transitions were assigned, connecting four low levels with A^+ symmetry to three levels with A^- symmetry. The stack with

A^- symmetry was observed for the first time. This stack is the lowest energy stack with A^- symmetry and defines the frequency of the geared bending mode of the $^{12}\text{C}^{18}\text{O}$ dimer at 3.607 cm^{-1} , a value which is smaller than that of the normal isotope, 3.731 cm^{-1} ,⁹ and that of the ^{13}C substituted isotope, 3.769 cm^{-1} .²⁹ New rovibrational calculations were made with the hybrid CO–CO potential of Ref. 13 in order to explain the effects of isotopic substitutions in the CO dimer. The results of these calculations agree very well with experiment, for all isotopologs. It was shown that not only a direct mass effect in the kinetic energy of the dimer, but also the change in anisotropy of the intermolecular potential with respect to the shifted monomer centers of mass, plays an essential role in the CO dimer. A similar effect of the anisotropy of the potential for isotopic shifts in weakly bound dimers has recently been found for He–CO (Ref. 33) and for HCN–HCl.³⁴

ACKNOWLEDGMENTS

This work was supported by the Forschungsgruppe Laborastronomie (FGLA). The work of three of the authors (D.N.F., V.A.P., and B.S.D.) at Cologne was made possible by the DFG through a grant aimed to support Eastern and Central European Countries and Republics of the FSU (436RUS113/719/0-2) and through the Leonhard-Euler Fellowship Program by the DAAD (05/05875). The support of the Russian Foundation for Basic Research (RFBR) (06-02-16035 and 05-02-04008) is gratefully acknowledged by three of the authors (L.A.S., B.S.D., and V.A.P.).

TABLE V. Calculated energy difference between the origins of the a and c stacks and intermolecular distances R_{eff} for these stacks, for different isotopologs of the CO dimer. The values for $(^{12}\text{C}^{18}\text{O})_2$ and $(^{13}\text{C}^{16}\text{O})_2$ in parentheses are from calculations with the $(^{12}\text{C}^{16}\text{O})_2$ potential expressed in the coordinates R , θ_A , θ_B , and ϕ without adjustment for the shift in the monomer centers of mass.

| | $(^{12}\text{C}^{16}\text{O})_2$ | $(^{12}\text{C}^{18}\text{O})_2$ | $(^{13}\text{C}^{16}\text{O})_2$ |
|-------------------------------------|----------------------------------|----------------------------------|----------------------------------|
| $(E_c - E_a)$ (cm^{-1}) | 0.89 | 0.64 (0.93) | 1.24 (0.95) |
| $R_{\text{eff},a}$ (\AA) | 4.344 | 4.313 (4.409) | 4.424 (4.409) |
| $R_{\text{eff},c}$ (\AA) | 4.108 | 4.118 (4.046) | 4.046 (4.052) |

- ¹P. A. Vanden Bout, J. M. Steed, L. S. Bernstein, and W. Klemperer, *Astrophys. J.* **234**, 503 (1979).
- ²M. Havenith, M. Petri, C. Lubina, G. Hilpert, and W. Urban, *J. Mol. Spectrosc.* **167**, 248 (1994).
- ³D. A. Roth, M. Hepp, I. Pak, and G. Winnewisser, *Chem. Phys. Lett.* **298**, 381 (1998).
- ⁴M. D. Brookes and A. R. W. McKellar, *Chem. Phys. Lett.* **287**, 365 (1998).
- ⁵M. D. Brookes and A. R. W. McKellar, *J. Chem. Phys.* **111**, 7321 (1999).
- ⁶D. A. Roth, L. A. Surin, B. S. Dumesh, G. Winnewisser, and I. Pak, *J. Chem. Phys.* **113**, 3034 (2000).
- ⁷K. A. Walker, C. Xia, and A. R. W. McKellar, *J. Chem. Phys.* **113**, 6618 (2000).
- ⁸K. A. Walker and A. R. W. McKellar, *J. Mol. Spectrosc.* **208**, 209 (2001).
- ⁹J. Tang, A. R. W. McKellar, L. A. Surin, D. N. Fourzikov, B. S. Dumesh, and G. Winnewisser, *J. Mol. Spectrosc.* **214**, 87 (2002).
- ¹⁰B. S. Dumesh, V. A. Panfilov, L. A. Surin, D. N. Fourzikov, and G. Winnewisser, *JETP Lett.* **80**, 98 (2004).
- ¹¹L. A. Surin, D. N. Fourzikov, F. Lewen, B. S. Dumesh, G. Winnewisser, and A. R. W. McKellar, *J. Mol. Spectrosc.* **222**, 93 (2003).
- ¹²G. W. M. Vissers, P. E. S. Wormer, and A. van der Avoird, *Phys. Chem. Chem. Phys.* **5**, 4767 (2003).
- ¹³G. W. M. Vissers, A. Heßelmann, G. Jansen, P. E. S. Wormer, and A. van der Avoird, *J. Chem. Phys.* **122**, 054306 (2005).
- ¹⁴A. van der Pol, A. van der Avoird, and P. E. S. Wormer, *J. Chem. Phys.* **92**, 7498 (1990).
- ¹⁵P. R. Bunker, P. Jensen, S. C. Althorpe, and D. C. Clary, *J. Mol. Spectrosc.* **157**, 208 (1993).
- ¹⁶A. W. Meredith and A. J. Stone, *J. Phys. Chem. A* **102**, 434 (1998).
- ¹⁷M. Rode, J. Sadlej, R. Moszynski, P. E. S. Wormer, and A. van der Avoird, *Chem. Phys. Lett.* **314**, 326 (1999).
- ¹⁸T. B. Pedersen, B. Fernández, and H. Koch, *Chem. Phys. Lett.* **334**, 419 (2001).
- ¹⁹M. Rode, J. Sadlej, R. Moszynski, P. E. S. Wormer, and A. van der Avoird, *Chem. Phys. Lett.* **334**, 424 (2001).
- ²⁰J. Fiser, T. Boublík, and R. Polák, *Mol. Phys.* **101**, 3409 (2003).
- ²¹P. R. Bunker and P. Jensen, *Molecular Symmetry and Spectroscopy*, 2nd ed. (NRC Research, Ottawa, 1998).
- ²²A. van der Avoird, P. E. S. Wormer, and R. Moszynski, *Chem. Rev. (Washington, D.C.)* **94**, 1931 (1994).
- ²³G. W. M. Vissers, G. C. Groenenboom, and A. van der Avoird, *J. Chem. Phys.* **119**, 277 (2003).
- ²⁴G. W. M. Vissers, G. C. Groenenboom, and A. van der Avoird, *J. Chem. Phys.* **119**, 286 (2003).
- ²⁵G. W. M. Vissers, L. Oudejans, R. E. Miller, G. C. Groenenboom, and A. van der Avoird, *J. Chem. Phys.* **120**, 9487 (2004).
- ²⁶C. Leforestier, L. B. Braly, K. Liu, M. J. Elrod, and R. J. Saykally, *J. Chem. Phys.* **106**, 8527 (1997).
- ²⁷G. C. Groenenboom, P. E. S. Wormer, A. van der Avoird, E. M. Mas, R. Bukowski, and K. Szalewicz, *J. Chem. Phys.* **113**, 6702 (2000).
- ²⁸A. R. W. McKellar, *J. Chem. Phys.* **115**, 3571 (2001).
- ²⁹L. A. Surin, D. N. Fourzikov, B. S. Dumesh, G. Winnewisser, J. Tang, and A. R. W. McKellar, *J. Mol. Spectrosc.* **223**, 132 (2004).
- ³⁰Y. J. Xu and W. Jäger, *J. Chem. Phys.* **111**, 5754 (1999).
- ³¹A. R. W. McKellar, *J. Mol. Spectrosc.* **226**, 190 (2004).
- ³²L. A. Surin, B. S. Dumesh, F. Lewen, D. A. Roth, V. P. Kostromin, F. S. Rusin, G. Winnewisser, and I. Pak, *Rev. Sci. Instrum.* **72**, 2535 (2001).
- ³³K. von Haeften, S. Rudolph, I. Simanovski, M. Havenith, R. E. Zillich, and K. B. Whaley, *Phys. Rev. B* **73**, 054502 (2006).
- ³⁴A. van der Avoird, T. B. Pedersen, G. S. F. Dhont, B. Fernández, and H. Koch, *J. Chem. Phys.* **124**, 204315 (2006).